

# Single atom alloy Ir/Ni catalyst boosts CO<sub>2</sub> methanation via mechanochemistry

Rui Tu,<sup>#</sup> Yujie Zhang,<sup>#</sup> Yuchun Xu, Junxia Yang, Ling Zhang, Keran Lv, Guoqing Ren,

Shengliang Zhai, Tie Yu,\* Weiqiao Deng\*

## Preparation of the Ir/Ni alloy catalyst

Ni ball is purchased from Yalian company with diameter of 10 mm and weight of 3.5~4.5 g. Prior to Ir impregnation, the Ni balls were firstly sonicated in ethanol for 30 min and washed with deionized water. And then the clean Ni ball was soaked in chloro-iridic acid solution (0.7 mM) for 10 h, followed by filtration, drying in air for 30 min, calcination at 850 °C for 2 h and reduction at 700 °C for 2 h under 20 mL min<sup>-1</sup> 10% H<sub>2</sub>/Ar. The ICP result showed 333 g Ni balls contained 0.0353 mg Ir content.

## Preparation of the Ni-Ir/Al<sub>2</sub>O<sub>3</sub> alloy

Al<sub>2</sub>O<sub>3</sub> ball is purchased from Aladdin with a weight of 0.4~0.5 g and a diameter of 10 mm. Prior to metal impregnation, the Al<sub>2</sub>O<sub>3</sub> balls were stirred in deionized water for 30 min. After drying the cleaned Al<sub>2</sub>O<sub>3</sub> balls, they were immersed in a chloro-iridic acid solution (0.016 M) and nickel nitrate solution (1.066 M) for 10 h, followed by filtration, drying in air for 30 min, calcination at 400 °C for 6 h and reduction at 400 °C for 3 h under 20 mL min<sup>-1</sup> 10% H<sub>2</sub>/Ar.

## Sample characterization

X-ray diffraction (XRD) patterns were recorded on a PANalytical Model Xpert3 instrument equipped with a Cu K $\alpha$  radiation source ( $\lambda = 0.15406$  nm) operating at 40

kV and 10 mA. X-ray photoelectron spectroscopy (XPS) was performed using a Thermo Fisher ESCALAB 250Xi spectrometer with a monochromatized Al K $\alpha$  X-ray source (1486.6 eV) and an applied power of 150 W. The C 1s (binding energy 284.6 eV) was used as a reference. Ir and Ni loading were estimated by inductively coupled plasma–optical emission spectrometry (Agilent 725 ICP–OES). SEM investigations were performed with a Quanta 250 FEG instrument to study the morphology of the metal surface. The elements mapping experiment was conducted on Thermo Scientific Apreo S Hivac instrument. The element mapping from XPS spectra were acquired with Thermo Scientific Nexsa instrument. The X-ray absorption spectra (XAS) of Ir L edge were collected at the beamline of TPS44A1 in National Synchrotron Radiation Research Center (NSRRC), Taiwan. The spectra were recorded under room temperature with fluorescence mode with a solid-state detector. TGA was conducted on a NETZSCH thermogravimetric analyzer (STA 449 F5) equipped with a Mettler-Toledo balance. Time-of-flight secondary ion mass spectrometry (TOF-SIMS) full spectra are used to study Ir spatial localization on Ir/Ni sample with lateral resolution to the sub 50 nm region. The depth profiling was performed on a TOF-SIMS 5-100 instrument (ION-TOF) GmbH, Münster, Germany) using a 30-KeV Bi $_3^+$  as analysis beam and 1-keV Cs $^+$  (O $_2^+$ ) as sputter source for positive (negative) polarity measurements. The analysis beam current was 0.7 pA, and the raster size was 50\*50  $\mu\text{m}^2$ . Incident angles of all beams are 45°. The DRIFTS spectra were collected on Bruker VERTEX 70v in the range of 650-4000  $\text{cm}^{-1}$  with a resolution of 4  $\text{cm}^{-1}$ . Prior to each test, the powder sample was pretreated with Ar at 350 °C for 0.5 h, and

its absorbance spectra were collected at RT as the background. The total flow rate was 25 mL/min for DRIFTS experiment, 5 mL/min CO<sub>2</sub> + 20 mL/min Ar for CO<sub>2</sub> adsorption and 2 mL/min CO<sub>2</sub> + 8 mL/min H<sub>2</sub> + 20 mL/min Ar for CO<sub>2</sub> methanation.

### **Activity test**

CO<sub>2</sub> methanation is performed by a homemade mechanical reactor with an electromotor used to control the vibration frequency of the reactor (Fig. 1a); the system could support mechanical reaction under 450 °C and vibration frequencies from 0~1500 rpm (motor speed). Typically, ~300 g Ni balls are sealed in the reactor, and the temperature is controlled with a type K thermocouple inserted inside the reactor. The feed gas is CO<sub>2</sub>: H<sub>2</sub>: N<sub>2</sub>=1: 4: 45. The reaction is performed at atmospheric pressure. Detailed procedures for each activity test are shown in the figure caption. The products are analyzed by online GC (ThermoFisher Trace 1300), which involves a thermal conductivity detector (TCD) and a flame ionization detector (FID). Porapak Q and 5 Å molecular sieve columns are connected to the TCD, while TG WAXMS and HP AL/S capillary columns are connected to the FID. Hydrocarbons are analyzed by FID, while CO<sub>2</sub>, Ar, CO and CH<sub>4</sub> are analyzed by TCD. CH<sub>4</sub> is taken as a reference to bridge between FID and TCD. The first sample test is recorded after 10 min of run time. CO<sub>2</sub> conversion and CH<sub>4</sub> selectivity are calculated as follows:

$$CO_2 \text{ conversion} = \frac{CO_2 \text{ inlet} - CO_2 \text{ outlet}}{CO_2 \text{ inlet}} \times 100\%$$

where CO<sub>2</sub> inlet and CO<sub>2</sub> outlet represent moles of CO<sub>2</sub> at the inlets and outlets, respectively.

$$CH_4 \text{ Selectivity} = \left(1 - \frac{CO \text{ outlet}}{CO_2 \text{ inlet}}\right) \times 100\%$$

where CO outlet represent moles of CO at the outlets. Since no other carbonaceous products are detected, the selectivity of CH<sub>4</sub> is calculated by the CO concentrations.

For Ir-Ni/Al<sub>2</sub>O<sub>3</sub> sample, ~56 g catalyst was packaged for the CO<sub>2</sub> methanation test to ensure the same volume of milling balls in the vessel.

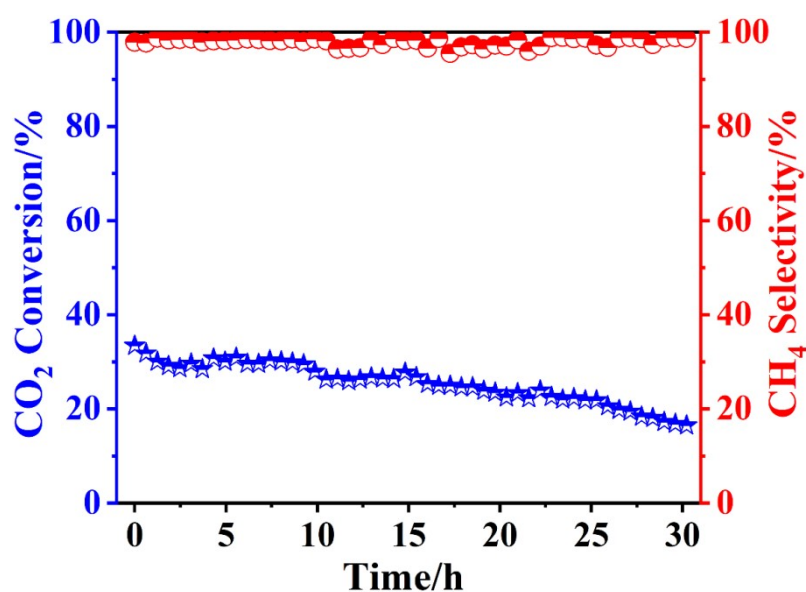


Figure S1 (a) The catalytic activity of Ir-Ni/Al<sub>2</sub>O<sub>3</sub> catalysts. Reaction conditions: 56 g catalyst, 350 °C, 800 rpm and 100 mL/min flow rate.

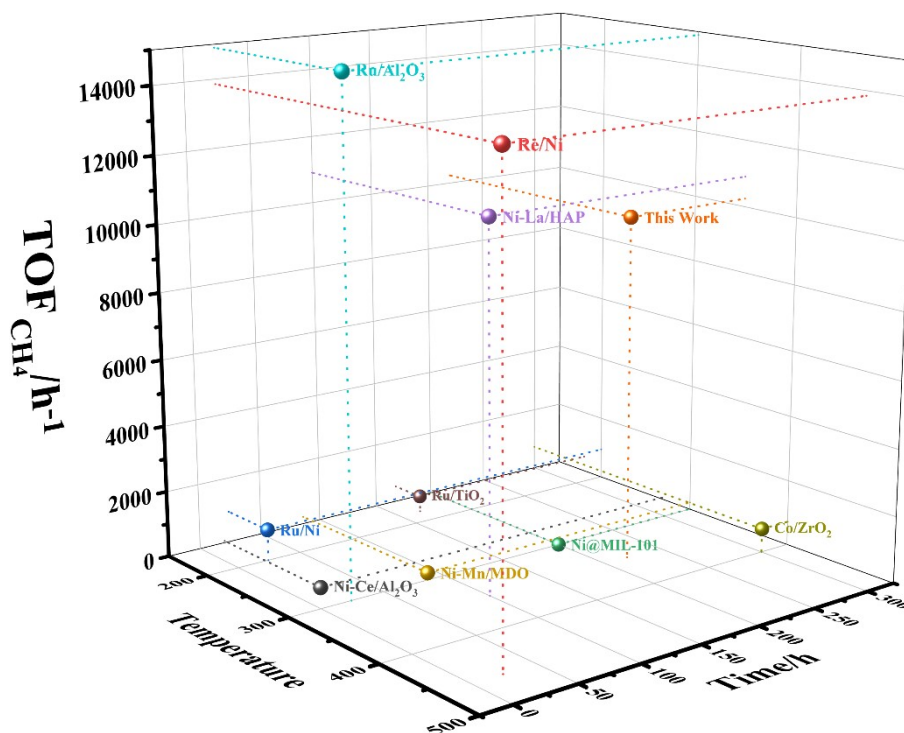


Figure S2 The comparison of desired reaction temperature-lifetime (h)-TOF<sub>CH<sub>4</sub></sub> (h<sup>-1</sup>) of representative CO<sub>2</sub> methanation catalysts.<sup>1-8</sup> 3D plot of catalysts lifetime and TOF<sub>CH<sub>4</sub></sub>, illustrating the balance of catalyst performance and stability over selected samples. At the present temperature, the catalysts exhibited the highest CO<sub>2</sub> conversion in literatures.

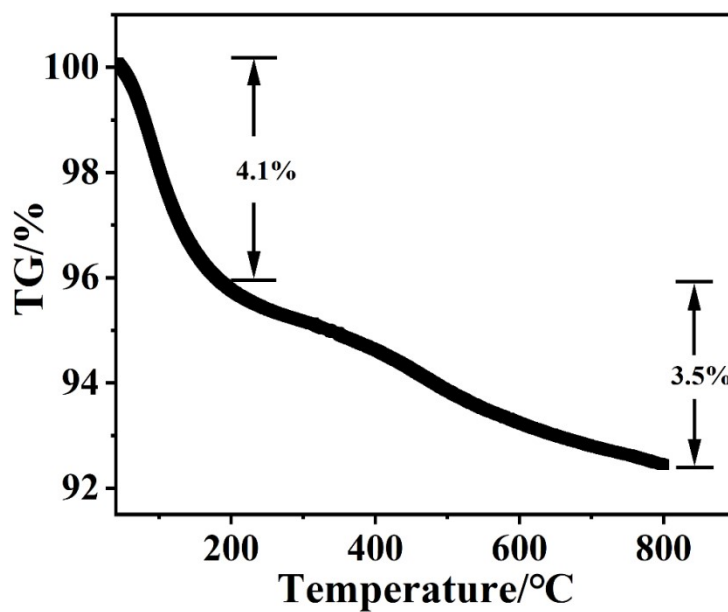


Figure S3 The weight loss profile of used Ir-Ni/Al<sub>2</sub>O<sub>3</sub> from thermogravimetric test

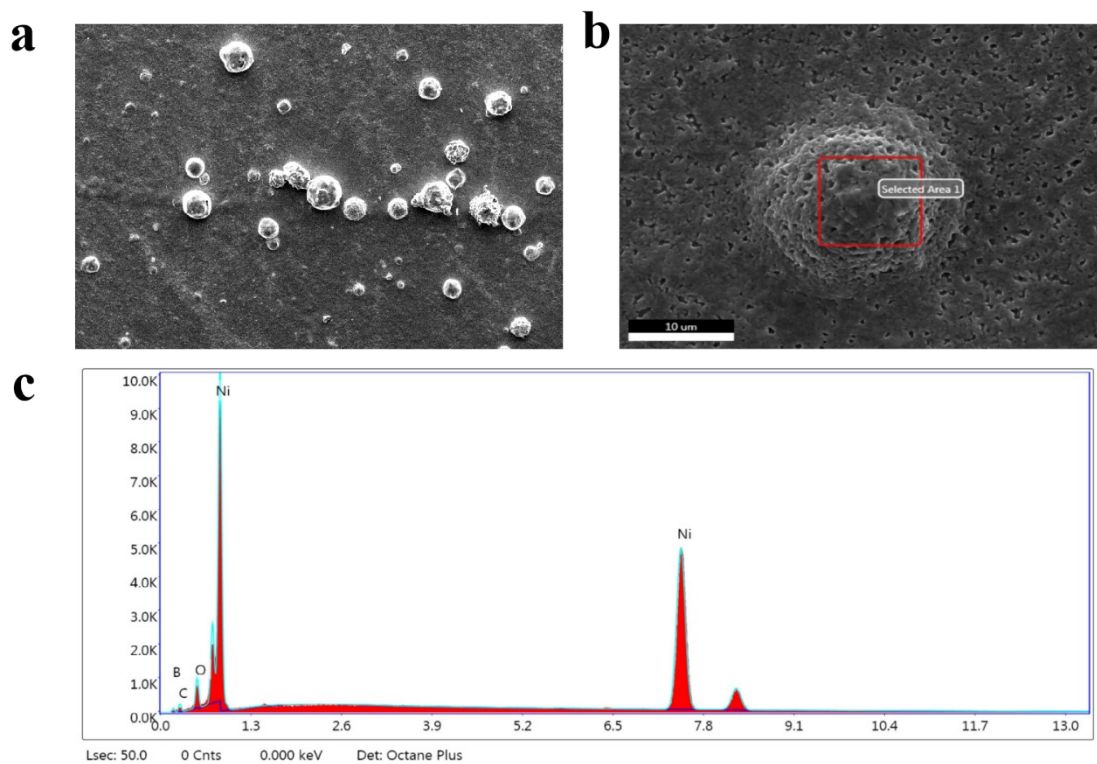


Figure S4. (a) Some spherical particles on used Ir/Ni metal surface from SEM results. (b) Exaggerated image of spherical particles on Ir/Ni metal surface. (c) EDS spectra of the spherical particle labelled by red square

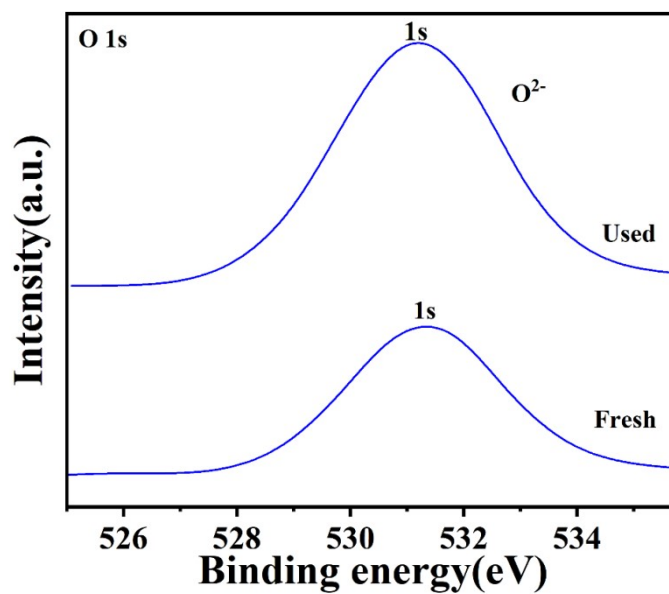


Figure S5 O 1s XPS spectra of fresh and used Ir/Ni

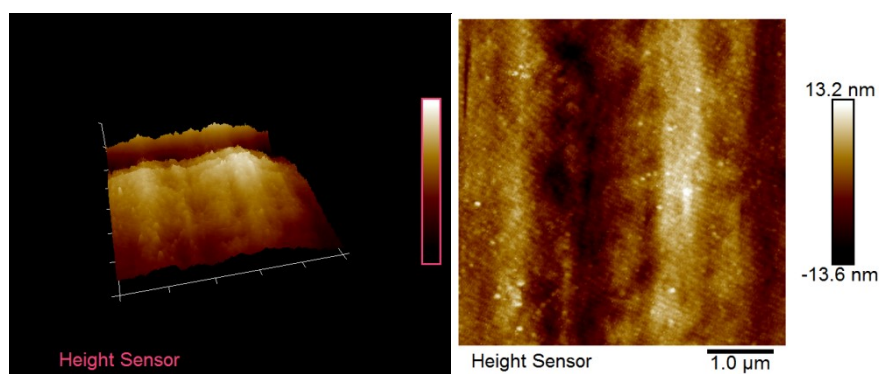


Figure S6 The 3D (left) and 2D (right) surface geometry images of fresh Ir/Ni sample from AFM, and the scale bar was -13.6~13.2 nm.

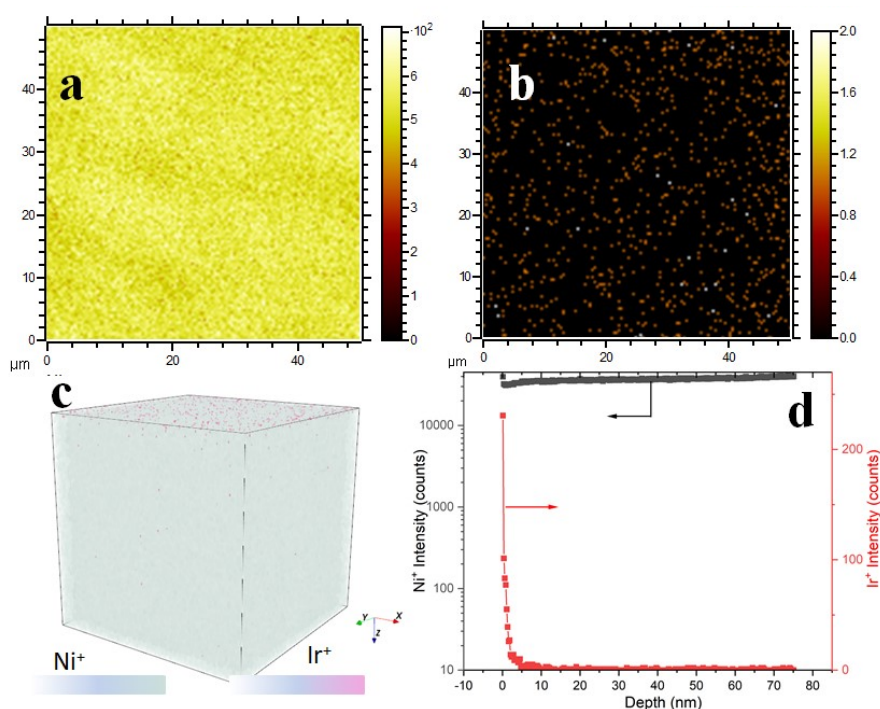


Figure S7 Images of elemental spatial distribution on spent Ir/Ni sample. The abundance maps of (a)  $\text{Ni}^+$  and (b)  $\text{Ir}^+$  over a  $50 \times 50 \mu\text{m}^2$  field of view from the Ir/Ni surface region. (c) The 3D TOF-SIMS map of Ir signal on the Ni substrate. (d) The  $\text{Ni}^+$  and  $\text{Ir}^+$  signals obtained by TOF-SIMS analysis with respect to the diffusion depth.

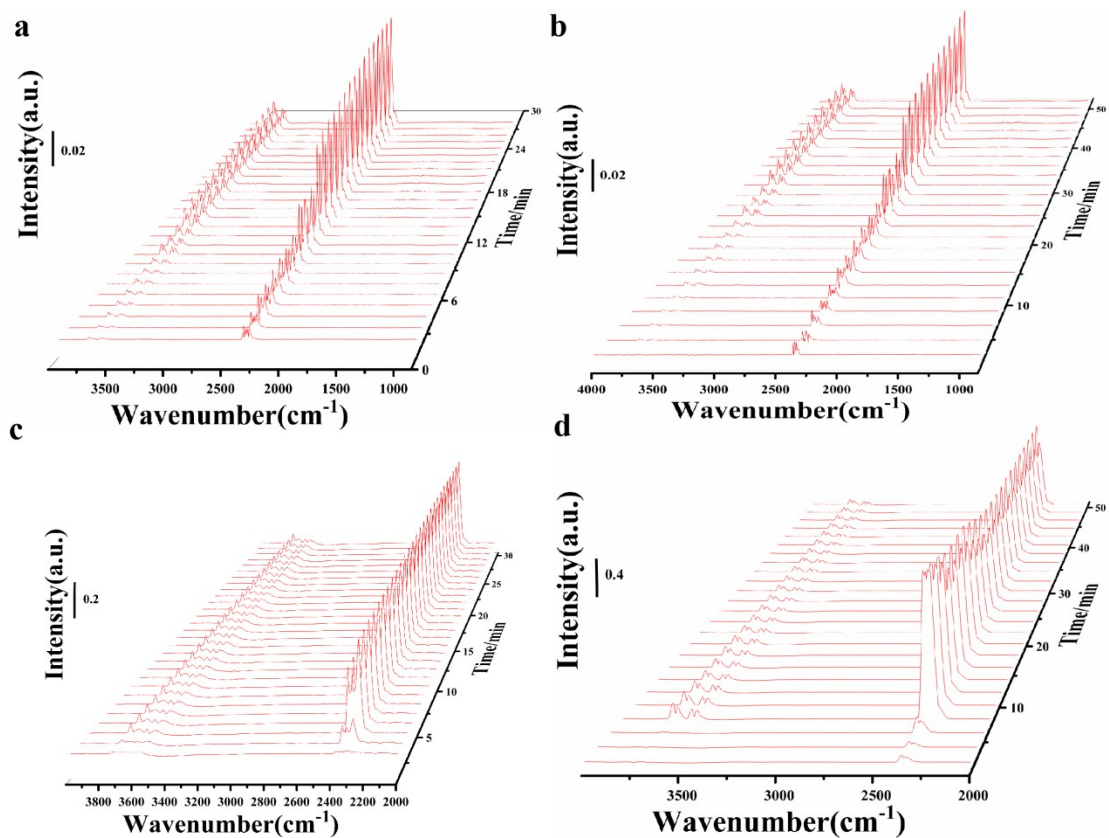


Figure S8 The DRIFTS results of CO<sub>2</sub> adsorption and CO<sub>2</sub>+H<sub>2</sub> reaction over Ni and Ir/Ni catalysts. (a) The CO<sub>2</sub> adsorption over Ni sample at 25 °C. (b) The CO<sub>2</sub> adsorption over Ir/Ni sample at 25 °C. (c) CO<sub>2</sub>+H<sub>2</sub> reaction over Ni sample at 150 °C. (d) CO<sub>2</sub>+H<sub>2</sub> reaction over Ir/Ni sample at 150 °C.

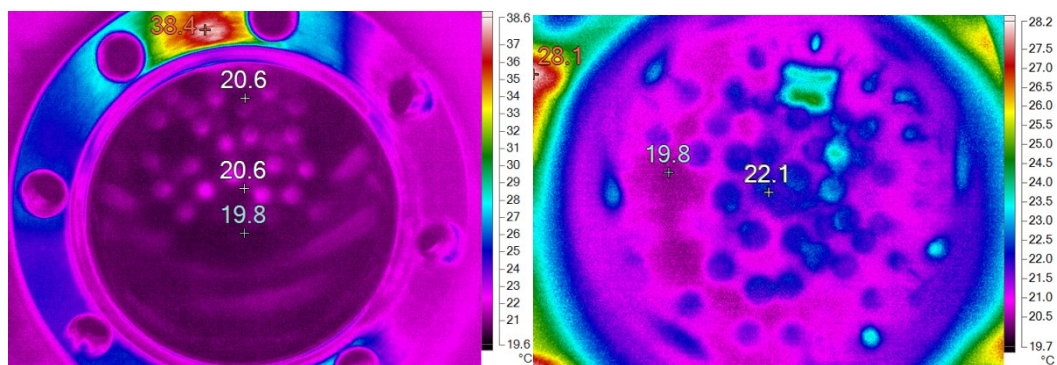


Figure S9 The temperature comparison of reaction system before (left) and after (right) 30 min collision under 1000 Hz vibration frequency by infrared camera.

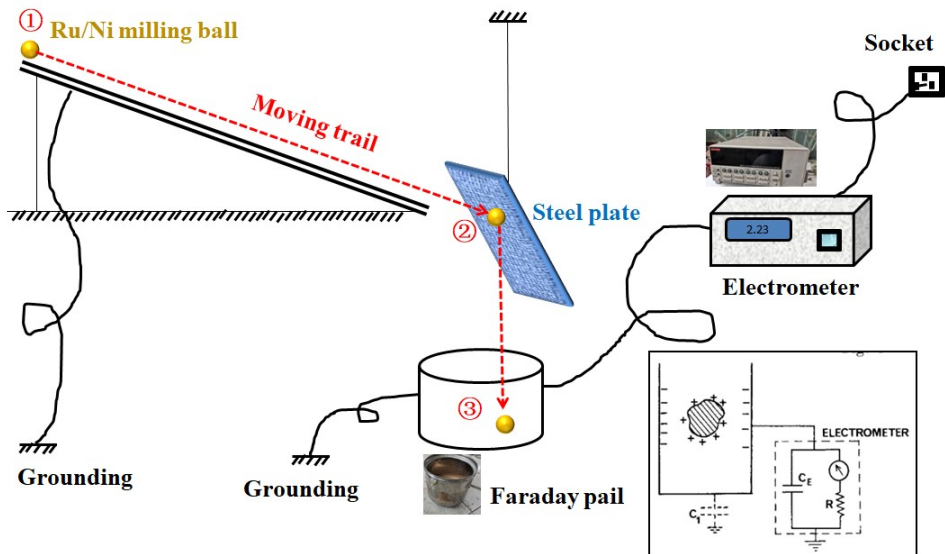


Figure S10 The schematic diagram of electric charge evaluation by faraday pail and the Ir/Ni was exemplified to show the collision trail between milling ball and steel plate.

The collisional electric charge was recorded Faraday pail and transformed into data results from electrometer, and the schematic diagram of built collision system utilizing Ir/Ni ball (Diameter = 10 mm) and steel plate as shown in Fig. S8. The repeat tests in Fig. S9 revealed the Ir/Ni milling balls possessed much higher charge than Ni balls, illustrating the doped Ir species improved the electric charge of Ir/Ni after mechanical collision compared with Ni ball.

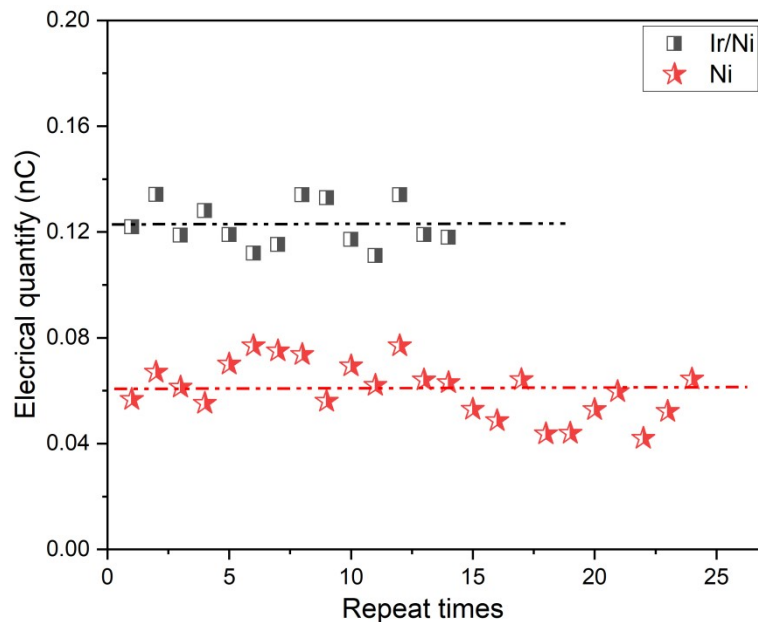


Figure S11 The electric charge on milling ball after collision with steel plate as a function of test times

**Table S1.** EXAFS fitting parameters at the Ir L-edge for various samples ( $S_0^2=0.70$ )

| Sample      | Shell | CN <sup>a</sup> | R(Å) <sup>b</sup> | $\sigma^2(\text{Å}^2)$ <sup>c</sup> | $\Delta E_0(\text{eV})$ <sup>d</sup> | R factor |
|-------------|-------|-----------------|-------------------|-------------------------------------|--------------------------------------|----------|
| Ir foil     | Ir-Ir | 12              | 2.70±0.01         | 0.003±0.0005                        | 9.40±1.46                            | 0.004    |
| Fresh Ir/Ni | Ir-Ni | 5.97±0.7<br>8   | 2.41±0.01         | 0.002±0.0007                        | 8.73±1.85                            | 0.005    |

<sup>a</sup>CN, coordination number; <sup>b</sup>R, distance between absorber and backscatter atoms; <sup>c</sup> $\sigma^2$ , Debye-Waller factor to account for both thermal and structural disorders; <sup>d</sup> $\Delta E_0$ , inner potential correction; R factor indicates the goodness of the fit.  $S_0^2$  was fixed to 0.70, according to the experimental EXAFS fit of Ir foil by fixing CN as the known crystallographic value.

## Reference

1. Michalska, K.; Kowalik, P.; Próchniak, W.; Borowiecki, T., Methanation at Very Low CO<sub>x</sub>/H<sub>2</sub> Ratio: Effect of Ce on Ni–Ce–Al Catalyst Properties and Empirical Kinetics. *Catalysis Letters* **2019**, *149* (1), 338-346.
2. Polanski, J.; Siudyga, T.; Bartczak, P.; Kapkowski, M.; Ambrozkiwicz, W.; Nobis, A.; Sitko, R.; Klimontko, J.; Szade, J.; Lelaćko, J., Oxide passivated Ni-supported Ru nanoparticles in silica: A new catalyst for low-temperature carbon dioxide methanation. *Applied Catalysis B: Environmental* **2017**, *206*, 16-23.
3. Zhen, W.; Gao, F.; Tian, B.; Ding, P.; Deng, Y.; Li, Z.; Gao, H.; Lu, G., Enhancing activity for carbon dioxide methanation by encapsulating (111) facet Ni particle in metal–organic frameworks at low temperature. *Journal of Catalysis* **2017**, *348*, 200-211.
4. Swalus, C.; Jacquemin, M.; Poleunis, C.; Bertrand, P.; Ruiz, P., CO<sub>2</sub> methanation on Rh/ $\gamma$ -Al<sub>2</sub>O<sub>3</sub> catalyst at low temperature: “In situ” supply of hydrogen by Ni/activated carbon catalyst. *Applied Catalysis B: Environmental* **2012**, *125*, 41-50.
5. Xiao, X.; Wang, J.; Li, J.; Dai, H.; Jing, F.; Liu, Y.; Chu, W., Enhanced low-temperature catalytic performance in CO<sub>2</sub> hydrogenation over Mn-promoted NiMgAl catalysts derived from quaternary hydroxalcalite-like compounds. *International*

*Journal of Hydrogen Energy* **2021**, *46* (66), 33107-33119.

6. Quindimil, A.; De-La-Torre, U.; Pereda-Ayo, B.; Davó-Quiñonero, A.; Bailón-García, E.; Lozano-Castelló, D.; González-Marcos, J. A.; Bueno-López, A.; González-Velasco, J. R., Effect of metal loading on the CO<sub>2</sub> methanation: A comparison between alumina supported Ni and Ru catalysts. *Catalysis Today* **2020**, *356*, 419-432.
7. Abe, T.; Tanizawa, M.; Watanabe, K.; Taguchi, A., CO<sub>2</sub> methanation property of Ru nanoparticle-loaded TiO<sub>2</sub> prepared by a polygonal barrel-sputtering method. *Energy & Environmental Science* **2009**, *2* (3), 315-321.
8. Li, W.; Nie, X.; Jiang, X.; Zhang, A.; Ding, F.; Liu, M.; Liu, Z.; Guo, X.; Song, C., ZrO<sub>2</sub> support imparts superior activity and stability of Co catalysts for CO<sub>2</sub> methanation. *Applied Catalysis B: Environmental* **2018**, *220*, 397-408.